Influence of evanescent waves on spin polarization in a ballistic Rashba bar

Zhongyao Li and Zhongqin Yang*
Surface Physics Laboratory (National Key Laboratory), Fudan University, Shanghai 200433, China
(Received 26 January 2007; revised manuscript received 1 May 2007; published 30 July 2007)

The influence of evanescent waves on spin polarization in a ballistic Rashba bar is investigated by solving continuous Schrödinger equations based on the expansion of evanescent waves as well as plane ones. We find that the pure evanescent waves can lead to obvious variations of spin polarization near the interfaces up to a range of several hundred nanometers. Both the range and strength of the variations are found to be strongly dependent on the incident energy. Due to the coupling between the evanescent waves and plane waves, and other factors, the influence of evanescent waves possesses long range behavior. The effects of evanescent waves on spin current and the possible relationship between spin current and polarization are also studied.

DOI: 10.1103/PhysRevB.76.033307 PACS number(s): 73.23.Ad, 72.25.Dc, 85.75.Nn

The evanescent wave (EW) in quantum mechanics describes an electron state with complex wave vector resulting when an electron tunnels through a potential barrier.[1] This state is an exponentially decaying state, which is much different from the propagating electron state described by real wave vectors. In solid systems, Kohn and Heine proposed the concept of "complex band structure" to describe the EW states.[2] The EWs have been found to be particularly important when electronic properties of solid surfaces or interfaces are considered, such as in semiconductor heterostructures, magnetic tunnel junctions, etc.[3–7]

Due to great potential applications in future spintronics, spin Hall effect[8–12] (SHE) has attracted considerable attention recently. Several theoretical groups[13–19] have focused on the theoretical study of current-induced spin polarization, also known as SHE,[16] in clean two-dimensional electron gases (2DEGs) with spin-orbit couplings (SOCs). Reynoso *et al.*[16] and Usaj and Balseiro[17] investigated analytically the influence of EWs on the spin polarization in a semi-infinite system with Rashba SOC. They found that the spin polarization in this case was dominated by the presence of evanescent modes, and its contribution decreases with the increase of the energy.[16] For a practical device, two leads are usually attached to a 2DEG with finite size. There must exist EWs at the interfaces between the leads and the sample. Yao and Yang have studied numerically the spin polarization in a 2DEG bar sandwiched between two leads based on the expansion of plane waves, but the effects of EWs are totally neglected there.[14] It is essential to study how the EWs affect the spin polarization in the system.

In this work, we explore the influence of EWs on spin polarization in a ballistic bar with Rashba SOC. Evanescent waves as well as plane waves are adopted to expand the wave functions of the system. We find the patterns of spin polarization to vary greatly if the EWs are considered. The pure EWs mainly affect the spin polarization near the interfaces. Both the range and strength of the EW influence are found to depend sensitively on the incident energy. They become larger (stronger) with the incident energy closer to a point where a new real channel opens up. The trend is much different from that obtained in a semi-infinite system.[16] Compared to the case without consideration of EWs, the variation on spin polarization induced by evanescent waves can extend to a long range because of the coupling of evanescent waves and plane waves, and other factors. The inclusion of EWs can improve the precision of the calculation.

We study current-induced spin polarization in a ballistic 2DEG bar with Rashba SOC.[20] The bar with a length of a is sandwiched between two semi-infinite leads along the x direction. The Hamiltonian of the structure investigated can be described by

$$\hat{H} = \left[\frac{\hat{p}_x^2 + \hat{p}_y^2}{2m^*} + V(y) \right] + \frac{\alpha}{\hbar}(\hat{p}_x\hat{\sigma}_y - \hat{p}_y\hat{\sigma}_x), \tag{1}$$

where m^* is the effective mass of electrons, α expresses the Rashba SOC strength, which is zero in the two leads, and $V(y)$ is the confined potential in the y direction. Open boundary is taken for the confined potential: $V(y)=0$ $(0<y<b)$, $V(y)=\infty$ $(y\leqslant 0;\ y\geqslant b)$, where b is the width of the bar and the leads. An electron wave is injected from the right lead to the left one, crossing the middle SOC region. The wave function in the SOC region can be written as

$$\psi_m(x,y) = \psi_{m1}(x,y)\begin{pmatrix}1\\0\end{pmatrix} + \psi_{m2}(x,y)\begin{pmatrix}0\\1\end{pmatrix},$$

where ψ_{m1} and ψ_{m2} can be expressed as

$$\psi_{m1}(x,y) = \sum_{n,k_x} C_{mn}(k_x)\sin\left(\frac{n\pi y}{b}\right)\exp(ik_x x)$$

and

$$\psi_{m2}(x,y) = \sum_{n,k_x} D_{mn}(k_x)\sin\left(\frac{n\pi y}{b}\right)\exp(ik_x x),$$

where $n=1,2,3,\ldots$. The number n expresses the confined energy levels, also called channels, due to the open boundary in the y direction. Note that the two-component wave function $(\psi_{m1}(x,y),\psi_{m2}(x,y))$ has been required to satisfy the hard-wall boundary condition in the y direction. Similarly, we can write the wave function in the right lead $(x>a)$ as

$$\psi_{mR}(x,y) = \sin\left(\frac{m\pi y}{b}\right)\exp(-ik_m x)\begin{pmatrix} s_1 \\ s_2 \end{pmatrix} + \sum_n A_{mn}\sin\left(\frac{n\pi y}{b}\right)\exp(ik_n x)\begin{pmatrix} 1 \\ 0 \end{pmatrix} + \sum_n B_{mn}\sin\left(\frac{n\pi y}{b}\right)\exp(ik_n x)\begin{pmatrix} 0 \\ 1 \end{pmatrix},$$

where $k_n = \sqrt{2m^* E/\hbar^2 - (n\pi/b)^2}$, and E is the incident energy. The first term in ψ_{mR} is the incoming wave incident from the mth channel, and $\binom{s_1}{s_2}$ expresses the spin state of the incident wave. The wave function in the left lead ($x<0$) has the form

$$\psi_{mL}(x,y) = \sum_n F_{mn}\sin\left(\frac{n\pi y}{b}\right)\exp(-ik_n x)\begin{pmatrix} 1 \\ 0 \end{pmatrix} + \sum_n G_{mn}\sin\left(\frac{n\pi y}{b}\right)\exp(-ik_n x)\begin{pmatrix} 0 \\ 1 \end{pmatrix}.$$

The expansion coefficients in the above wave functions can be determined uniquely from the Schrödinger equations and the continuous conditions of wave functions at the two interfaces between the sample and the leads.[14,21,22]

In our numerical calculations, we suppose an unpolarized incident electron wave, and do the statistical average for the spin polarization of each incident electron wave with energy E in each channel. The incident channel number can be selected as $m=1,2,\ldots,N_0$, where $N_0=[\sqrt{2m^* E}b/\pi\hbar]$ is the maximum number of channels with real wave vectors in the x direction. In order to consider the effects of evanescent waves, the confined energy levels considered can exceed the incident energy E, i.e., $n>N_0$. In this case, the imaginary wave vector in leads $k_n=\pm i\sqrt{(n\pi/b)^2-2m^* E/\hbar^2}$ (the complex wave vectors in the SOC bar can be obtained by solving the secular equations in the region), where $n=N_0+1$, $N_0+2,\ldots,N_0+\Delta n$. Δn gives the number of EWs considered. From the calculations, we find that only finite Δn, usually 4–5, needs to be included for a strip with fixed incident energy and width. We have confirmed that taking more EWs in the calculations does not change the results markedly. Those 4–5 EWs, however, have major influence not only on the numerical precision but also on the patterns of spin polarization. In the calculations, we usually take $m^*=0.04m_e$ and $E=15$ meV, except when stated explicitly.

To show the influence of EWs, we calculate spin polarization in the Rashba bar with and without the consideration of the EWs, respectively. Four EWs are considered in the calculation. Figures 1(a) and 1(b) give the contour plots of spin polarizations of $\langle S_x(x,y)\rangle$, $\langle S_y(x,y)\rangle$, and $\langle S_z(x,y)\rangle$ with and without the effects of EWs, respectively. Note that the magnitude of $\langle S_x(x,y)\rangle$ in the middle region of Fig. 1(a) is multiplied by a factor of 5 to compare well with Fig. 1(b). Comparing Figs. 1(a) and 1(b), it can be seen that the main characteristic of spin polarization of all $\langle S_x(x,y)\rangle$, $\langle S_y(x,y)\rangle$, and $\langle S_z(x,y)\rangle$ in the middle region, such as 100 nm$<x<$400 nm, remains even after the EWs are considered, although there are some differences in detail between the patterns in the region, especially for $\langle S_z(x,y)\rangle$. The phenomenon of the out-of-plane spin polarization $\langle S_z(x,y)\rangle$ with opposite signs near the lateral edges in nonmagnetic materials is known as the spin Hall effect.[10–12] After considering the EWs, the out-of-plane spin polarization $\langle S_z(x,y)\rangle$ (also for $\langle S_x(x,y)\rangle$ and $\langle S_y(x,y)\rangle$ to some extent) tends to oscillate strongly along the transversal direction in the middle region of the bar. The additional oscillations can be ascribed to constructive or destructive interferences between the EWs and plane waves or EWs and EWs in different channels in the bar.

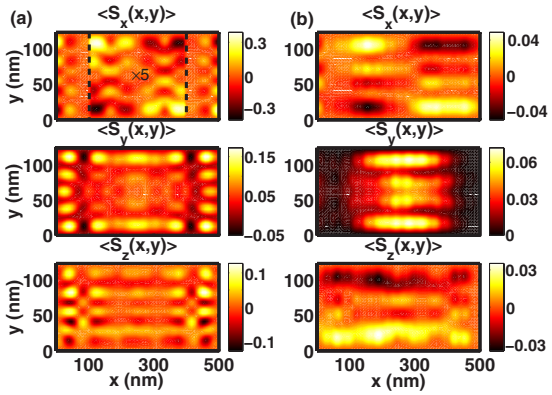

FIG. 1. (Color online) Contour plots of spin polarizations of $\langle S_x(x,y)\rangle$, $\langle S_y(x,y)\rangle$, and $\langle S_z(x,y)\rangle$ (in $\hbar/2$) in a Rashba bar (a) with and (b) without consideration of EWs. The strength of Rashba SOC is fixed at $\alpha=2.0\times10^{-11}$ eV m.

After considering EWs, the most notable variation in the spin polarization occurs near the interfaces between the sample and leads. The EWs in Fig. 1(a) give rise to very rich polarization patterns appearing near the two interfaces within about 100 nm. In the corresponding areas in Fig. 1(b), the distributions of spin polarization are more monotonous. All the patterns in Figs. 1(a) and 1(b) are found to satisfy "up-down" symmetries along the transversal direction,[14,16] while only the results obtained with the EWs obey the "left-right" symmetries along the longitudinal direction: $\langle S_x(x,y)\rangle=-\langle S_x(a-x,y)\rangle$ and $\langle S_{y,z}(x,y)\rangle=\langle S_{y,z}(a-x,y)\rangle$ [see Fig. 1(a)]. Actually, in linear region, the left-right symmetries are caused by the symmetry of the Hamiltonian in Eq. (1), $\hat{H}(\alpha,\sigma_x,\sigma_y)=\hat{H}(-\alpha,-\sigma_x,-\sigma_y)$, and the special bar geometry considered.[14,16] It can be inferred that the inclusion of evanescent waves can improve the precision of the numerical calculations.

In order to study the influence of EWs on spin polarization, we extract the contribution of pure complex wave vectors k_x to spin polarization, shown in Fig. 2. The two vertical lines at $x=0$ and 500 nm in the figure express the interfaces between the sample and leads. At the incident energy of 15 meV, the EWs have a drastic influence on the spin polarization near the interfaces in the range of 50 nm in the leads and 100 nm in the SOC region, illustrating well why the spin polarization near the interfaces in Fig. 1(a) varies enormously. It is also reasonable that the contribution of the pure EWs decays exponentially with the increase of the distance away from the interfaces. The spin polarization in leads in

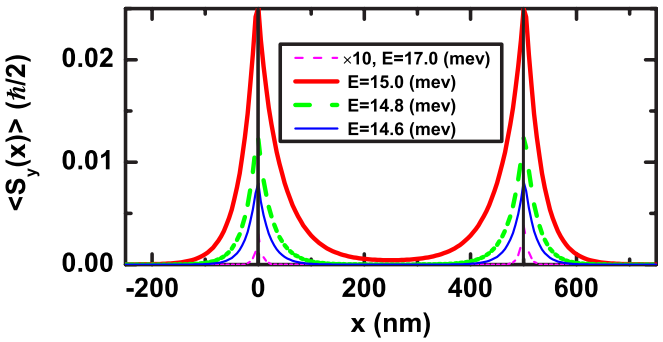

FIG. 2. (Color online) The contribution from pure EWs to spin polarization of $\langle S_y \rangle$ averaged in the y direction at different incident energies.

Fig. 2 comes from the reflected EWs. Their strengths are determined by the boundary conditions in the interfaces. From Fig. 2, it is known that the influence of EWs depends sensitively on the incident energy. It increases with the increase of the incident energy from 14.6 to 15.0 meV. This can be rationalized by $k_x \approx \pm i\sqrt{(n\pi/b)^2 - 2m^*E/\hbar^2}(n > N_0)$ in the Rashba region and the value of $|\mathrm{Im}[k_x]|$ will decrease with the increase of the energy for a fixed channel. The trend causes this EW to decay more slowly with the energy, and thus, contribute more to spin polarization. If the incident energy exceeds the confined energy level of the channel, the channel becomes a traveling state. It will not contribute any more to Fig. 2. Therefore, the contribution from the pure complex wave vectors drops and then it increases again with the further increase of the energy. This cyclical behavior can be seen easily from Fig. 2, when the energy increases to 17.0 meV, where a new real channel is opened. Similar relations can be found for $\langle S_x \rangle$ and $\langle S_z \rangle$ if the averages are taken for the half-width of the y direction. This property of EW strength is much different from the results obtained by Reynoso *et al.* for a semi-infinite system.[16] They found the

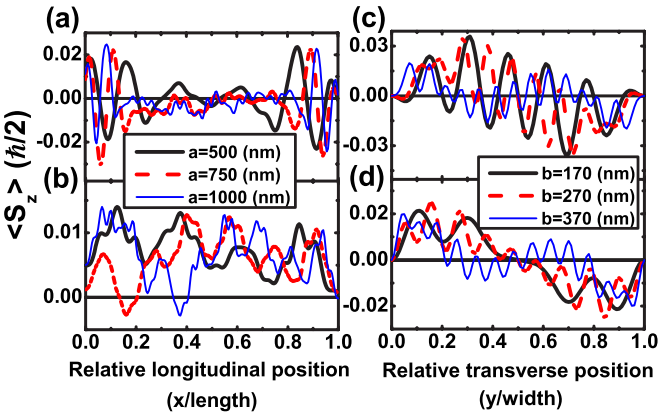

FIG. 3. (Color online) The average spin polarization of $\langle S_z \rangle$ as a function of the longitudinal position in the Rashba bar: (a) with consideration of EWs and (b) without consideration of EWs. Due to the "up-down" symmetry, the average is made only in the lower half plane (from $y=0$ to $y=b/2$). (c) and (d) are the average spin polarizations of $\langle S_z \rangle$ as a function of the lateral position in the Rashba bar with and without EWs considered, respectively.

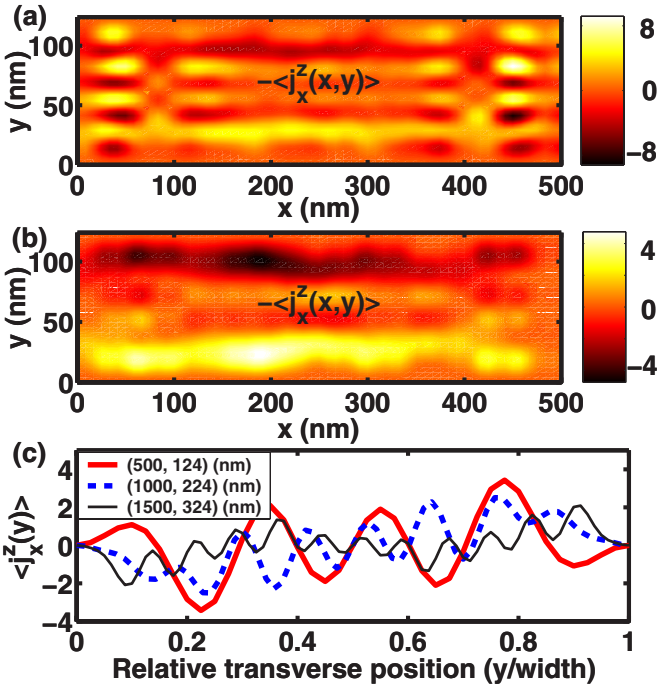

FIG. 4. (Color online) Contour plots of spin current $\langle j_x^z(x,y) \rangle$ (in $\hbar^2 m_e^{-1}$ bohr$^{-1} \times 10^{-3}$) (a) with EWs and (b) without EWs. The parameters used are the same as that in Fig. 1 (c) The average spin current of $\langle j_x^z \rangle$ (in $\hbar^2 m_e^{-1}$ bohr$^{-1} \times 10^{-3}$) as a function of the lateral position with different sample sizes of (a,b). The parameters a and b denote the length and the width of the sample, respectively.

contribution from EWs to decrease with the increase of the energy.[16] The difference can be ascribed to various models studied. In the semi-infinite system, the dispersive relationship of the two shifted parabolas in all directions causes the contribution of EWs to the spin polarization to be much larger at the low energy region and to decrease with the increase of energy. No confined potential appears in their model. Thus, there is no channel concept, giving rise to a non cyclical behavior of the contribution of EWs to spin polarization in their case.[16]

Since the influence of EWs shown in Fig. 2 decreases exponentially with the distance from the interfaces, its role will become less important when the length of the 2DEG bar is longer. However, there are mechanisms which can affect the spin polarization in long range. Due to the long-distance behavior of plane waves, the mixed terms of plane waves and evanescent ones can change the patterns of spin polarization for long distances. At the same time, the coupling equations of boundary conditions can be modulated because of the EWs considered. It will also cause the patterns of spin polarization to vary in a large range. These two mechanisms can illustrate the subtle variations of spin polarization in the middle region in Fig. 1(a) from that in Fig. 1(b). They will also lead to important pattern modifications even in a very long sample. Figure 3(a) shows the average (lower half plane) spin polarization of $\langle S_z \rangle$ with EWs at different sample lengths. The results without EWs are given in Fig. 3(b). The variation of $\langle S_z \rangle$ near the two interfaces in Fig. 3(a) comes from the pure EWs. Its range shrinks to the interfaces gradu-

ally with the increase of the length, because at a certain incident energy, the influence range of pure EWs is almost the same, about 100 nm, almost independent of the sample length. Compared to Fig. 3(b), the change in the middle region in Fig. 3(a) must be due to the long-distance mechanisms. Even in the case of $a=1000$ nm, $\langle S_z \rangle$ in the middle region is still much different in Figs. 3(a) and 3(b). In a very long Rashba bar, the long-distance mechanisms will cause the main differences in spin polarization with and without the consideration of EWs.

The effect of sample width on the spin polarization is shown in Figs. 3(c) and 3(d). The EWs are included in Fig. 3(c), but not in Fig. 3(d). Regardless of considering EWs or not, the main peaks with opposite magnitudes of the spin polarization can move gradually to the two lateral edges with the increase of the sample width. The strength of the peaks, however, depends on whether the EWs are considered. The strength in Fig. 3(c) decreases with the increase of the width, while there is no such trend in Fig. 3(d). With the increase of the width of the 2DEG bar, the average strengths of $\langle S_x(x,y) \rangle$ and $\langle S_y(x,y) \rangle$ along the transversal direction are also found to decrease after the EWs are included. Therefore, it can be inferred that in a much larger sample, the effect of spin polarization may become weak.

The influence of EWs on spin current is also studied. Figures 4(a) and 4(b) indicate the comparison of $\langle j_x^z(x,y) \rangle$ $\left[j_x^z = \frac{\hbar}{4}(\hat{\sigma}_z \hat{v}_x + \hat{v}_x \hat{\sigma}_z) \right]$ with and without inclusion of EWs. It is evident that the EWs modify the distribution of spin current not only in the region near the interfaces but also in the middle area of the sample, like the case of spin polarization. It is very interesting to note that the patterns of spin current $\langle j_x^z(x,y) \rangle$ shown in Figs. 4(a) and 4(b) are very similar to the spin polarization of $\langle S_z(x,y) \rangle$ (see Fig. 1). The minus signs of spin currents in Figs. 4(a) and 4(b) come from the negative velocity of electrons, which are injected from the right lead to the left one. However, the spin current $\langle j_y^z(x,y) \rangle$ flowing along the y direction is found not to be related to any of the spin polarization. It is obstructed at the two lateral edges due to the hard-wall boundary there. The analogy of $\langle j_x^z(x,y) \rangle$ with $\langle S_z(x,y) \rangle$ should be related to the fact that we inject a charge current along the x direction, and there is no net charge current in the y direction. The obtained relationship between spin current and polarization is quite different from that found in the presence of magnetic field,[23] where the spin current $\langle j_x^z \rangle$ is found to be proportional to $\langle S_y \rangle$. With the increase of the size of the structure, the spin current is found to decrease as seen in Fig. 4(c). This trend will also lead to the weakening of spin current in a large Rashba system, as the spin polarization does.

We have studied the influence of evanescent waves on spin polarization in a spin-orbit coupling bar connected with two semi-infinite leads. The evanescent waves can lead to obvious changes of the pattern of spin polarization not only in the regions near the interfaces but also in the middle region of a long sample due to different mechanisms. The contribution of pure evanescent waves to spin polarization is found to depend sensitively on the incident energy. The pattern of spin current $\langle j_x^z(x,y) \rangle$ is found to be very similar to that of spin polarization $\langle S_z(x,y) \rangle$ in a ballistic bar geometry.

This work was supported by the National Natural Science Foundation of China with Grant No. 1067027, the Grand Foundation of Shanghai Science and Technology (05DJ14003), PCSIRT, and 973 Project under Grant No. 2006CB921300.

*zyang@fudan.edu.cn

[1] E. Merzbacher, *Quantum Mechanics* (Wiley, New York, 1998).
[2] W. Kohn, Phys. Rev. **115**, 809 (1959); V. Heine, Proc. Phys. Soc. London **81**, 300 (1963).
[3] M. F. H. Schuurmans and G. W.'t Hooft, Phys. Rev. B **31**, 8041 (1985).
[4] G. Edwards and J. C. Inkson, Semicond. Sci. Technol. **9**, 310 (1994).
[5] Ph. Mavropoulos, N. Papanikolaou, and P. H. Dederichs, Phys. Rev. Lett. **85**, 1088 (2000).
[6] D. Stoeffler, J. Phys.: Condens. Matter **16**, 1603 (2004).
[7] J. K. Tomfohr and O. F. Sankey, Phys. Rev. B **65**, 245105 (2002).
[8] J. E. Hirsch, Phys. Rev. Lett. **83**, 1834 (1999).
[9] S. Zhang, Phys. Rev. Lett. **85**, 393 (2000).
[10] Y. K. Kato, R. C. Myers, A. C. Gossard, and D. D. Awschalom, Science **306**, 1910 (2004).
[11] J. Wunderlich, B. Kaestner, J. Sinova, and T. Jungwirth, Phys. Rev. Lett. **94**, 047204 (2005).
[12] N. P. Stern, S. Ghosh, G. Xiang, M. Zhu, N. Samarth, and D. D. Awschalom, Phys. Rev. Lett. **97**, 126603 (2006).
[13] B. K. Nikolić, S. Souma, L. P. Zârbo, and J. Sinova, Phys. Rev. Lett. **95**, 046601 (2005).
[14] J. Yao and Z. Q. Yang, Phys. Rev. B **73**, 033314 (2006).
[15] J. Wang, K. S. Chan, and D. Y. Xing, Phys. Rev. B **73**, 033316 (2006).
[16] A. Reynoso, Gonzalo Usaj, and C. A. Balseiro, Phys. Rev. B **73**, 115342 (2006).
[17] G. Usaj and C. A. Balseiro, Europhys. Lett. **72**, 631 (2005).
[18] Y. Jiang, Phys. Rev. B **74**, 195308 (2006).
[19] Q. Wang and L. Sheng, Int. J. Mod. Phys. B **19**, 4135 (2005).
[20] Y. A. Bychkov and E. I. Rashba, J. Phys. C **17**, 6039 (1984).
[21] T. Matsuyama, C.-M. Hu, D. Grundler, G. Meier, and U. Merkt, Phys. Rev. B **65**, 155322 (2002).
[22] Q.-F. Sun and X. C. Xie, Phys. Rev. B **71**, 155321 (2005).
[23] Yun-Juan Bao, Huai-Bing Zhuang, Shun-Qing Shen, and Fu-Chun Zhang, Phys. Rev. B **72**, 245323 (2005).